Evidence for a Light-Induced H^+ Conductance in the Eye of the Green Alga *Chlamydomonas reinhardtii*

Sabine Ehlenbeck,* Dietrich Gradmann,† Franz-Josef Braun,* and Peter Hegemann*
*Institut für Biochemie I, Universität Regensburg, 93040 Regensburg, Germany and †Abteilung Biophysik der Pflanze, Albrecht-von-Haller-Institut für Pflanzenwissenschaften der Universität, D-37073 Göttingen, Germany

ABSTRACT Rhodopsin-mediated photoreceptor currents, I_P, of the unicellular alga *Chlamydomonas reinhardtii* were studied under neutral and acidic conditions. We characterized the kinetically overlapping components of the first, flash-induced inward current recorded from the eye, I_{P1}, as a low- and high-intensity component, I_{P1a} and I_{P1b}, respectively. They peak between 1 and 10 ms after the light-flash and are both likely to be carried by Ca^{2+}. I_{P1a} and I_{P1b} exhibit half-maximal photon flux densities, $Q_{1/2}$, of ~0.14 and 58 $\mu E\ m^{-2}$, and maximal amplitudes of ~4.9 and 38 pA, respectively. At acidic extracellular pH values (pH 3–5), both I_{P1} currents are followed by distinct H^+ currents, I_{P2a} and I_{P2b}, with maxima after ~5 and 100 ms, respectively. Because the $Q_{1/2}$ values of I_{P1b} and I_{P2b} virtually coincide with $Q_{1/2}$ of rhodopsin bleaching, we suggest that the respective conductances G_{1b} and G_{2b} are closely coupled to the rhodopsin, whereas the low light-saturating conductances G_{1a} and G_{2a} reflect transducer-activated states of a second rhodopsin photoreceptor system.

INTRODUCTION

The eyes of unicellular flagellate algae contain one or more rhodopsin-type photoreceptors, which, upon light stimulation, evoke electrical inward currents within the eyespot area (photoreceptor currents, I_P) (Sineshchekov and Govorunova, 1999). These inward currents were recorded from *Hematococcus pluvialis* wild-type cells (Litvin et al. 1978) or from a cell wall-deficient *Chlamydomonas reinhardtii* mutant (Harz and Hegemann, 1991). In *C. reinhardtii* the small photoreceptor current I_P, saturated at low light, induces an asymmetrical change of the flagellar beating (Holland and Hegemann, unpublished). Because of the directional properties of the eye, the transient beat asymmetry occurs in such a way that the cells preferentially orient toward or away from the light source (Foster and Smyth, 1980; Rüffer and Nultsch, 1990). When the flash photon exposure exceeds a certain threshold, I_P is superimposed by a fast all-or-none flagellar current, I_{FF}, followed by a slow and small current-tail <1 pA, I_{FS}. It is clear that both flagellar current components are carried by Ca^{2+}, and that Ca^{2+} down-regulates I_{FS} from inside (Holland et al., 1996). I_{FF} is the current that causes the switch of the flagellar waveform from forward swimming to undulation (*stop response* or *photophobic response*), as shown by simultaneous recording of photocurrents and flagellar beating (Holland et al., 1997). The ion specificity of the photoreceptor current I_P and its signaling properties are less clear by far. I_P depends on extracellular Ca^{2+}, and in the early experiments on *C. reinhardtii*, I_P had disappeared completely at <0.1 μM Ca^{2+} (Harz and Hegemann, 1991). In other experiments on *H. pluvialis* and *C. reinhardtii*, 15 to 30% of the I_P persisted at Ca^{2+} levels below 1 nM (Sineshchekov, 1991; Holland et al., 1996). It could not be unequivocally clarified which ion carries the residual current. A supposedly Ca^{2+}-independent portion, I_{P1a}, and a Ca^{2+}-dependent component, I_{P1b}, have been discriminated since then ($I_P = I_{P1a} + I_{P1b}$) (Sineshchekov, 1991; Holland et al., 1996).

Because the more Ca^{2+}-sensitive component I_{P1b} dominates the photocurrent I_{P1} at high flash energies under otherwise physiological conditions, I_{P1b} was studied in more detail than I_{P1a} (Sineshchekov and Govorunova, 1999). I_{P1b} saturates only at very high flash intensities, it rises with a delay of <30 μs, and it peaks at ~1 ms after the flash. The short delay and the high saturation level originally lead to the suggestion that I_{P1b} is indicative of a charge redistribution within the rhodopsin photoreceptor and does not reflect translocation of ions, as in the early receptor potential of animal vison (Sineshchekov et al., 1990). This hypothesis, however, did not hold true for *C. reinhardtii* where I_{P1b} was assigned to a real inward current, for the following reasons. First, estimating 10 000 rhodopsin molecules per cell, ~100 charges will be displaced across the membrane per rhodopsin molecule (Harz et al., 1992). Second, in experiments with double flashes of moderate energy, the second flash could not evoke a photoreceptor current (Holland et al., 1996). To explain the short delay between flash and photocurrent rise we have proposed that the light-induced conductance for I_{P1b} is either closely linked to rhodopsin or is a light-activated form of rhodopsin itself (Harz et al., 1992; Holland et al., 1996).

Recording photoelectric responses in cell suspension and suction experiments with improved time resolution allowed the analysis of I_{P1} in response to dim flashes in *C. reinhardtii* and *Volvox carteri* (Sineshchekov et al., 1992; Holland et al., 1996; Braun and Hegemann, 1999a). At these low-light levels, I_{P1} is dominated by the less Ca^{2+}-sensitive component I_{P1a} (formerly named P_S). The delay time between flash and beginning of the photocurrent increased to

Submitted April 24, 2001, and accepted for publication October 11, 2001.
Address reprint requests to: Peter Hegemann, Institut für Biochemie I, Universität Regensburg, 93040 Regensburg, Germany. Tel.: 49-941-943-2814; Fax: 49-941-943-2936; E-mail: Peter.Hegemann@biologie.uni-regensburg.de

0006-3495/02/02/740/12 $2.00

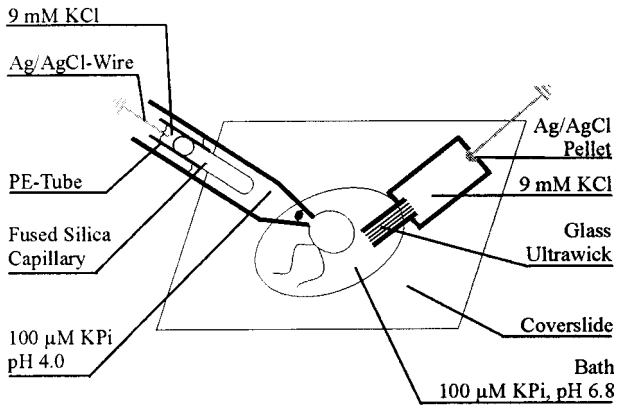

FIGURE 1 Experimental setup for current recordings in suction-pipette configuration with low (≈ 15 nM), external $[Ca^{2+}]$.

several milliseconds and the flash-to-peak time was accordingly extended up to 10 ms (Braun and Hegemann, 1999a). Extended delays and flash to peak times are especially evident in *V. carteri*, because all electrical responses are generally slower and I_{P1a} is more prominent in this colonial species as compared with its unicellular relatives. The observations were interpreted in terms of a second ionic process involving biochemical signal transduction processes.

Here we extend the characterization of the photoreceptor currents I_{P1a} and I_{P1b} in *C. reinhardtii*. In addition, we report on a new acid-induced photoreceptor current, I_{P2}. This current is slowly activated and appears with a large amplitude at acidic pH in response to brief flashes or, as a large stationary current, upon step-up stimulation.

MATERIALS AND METHODS

All experiments were carried out with the *C. reinhardtii* strain CW2 cells. Cells were converted into gametes in *N*-methyl-D-glucamine $(NMG)^+/K^+$-buffer (5 mM Hepes adjusted to pH 6.8 with NMG, 200 μM Ca^{2+}, 100 μM K^+, and 10 μM BAPTA) overnight.

Electrical measurements

CW2 cells were dark-adapted for more than 1 h before they were used for experiments. The NMG^+/K^+-buffer was used as electrode and bath solution. Ca^{2+} was added as $CaCl_2$. The total amount of Ca^{2+} required for a defined concentration of *free* Ca^{2+} was calculated according to Holland et al. (1996).

Ca^{2+}-free conditions were accomplished by using 100 μM KPi-buffer. The buffer was prepared from bi-deionized H_2O finally poured through a strong acid cation exchange resin (Dowex-50 W, Sigma, St. Louis, MO). The buffer was adjusted to pH 6.8, the Ca^{2+} concentration was measured using Fura-2 (Molecular Probes, Eugene, OR), and the buffer was finally adjusted to the desired pH by titration with ultrapure HCl (Merck, Darmstadt, Germany). The gametes were washed three times in KPi-buffer and stored in the dark. Because of the low ionic strength of the KPi-buffer, electrodes were kept in 9 mM KCl and separated by salt bridges as illustrated in Fig. 1. The fused silica capillary used for the pipette electrode had a diameter of 300 μm (o.d., TSP 180350, Composite Metal Services, Worcester, UK).

Suction pipette measurements

Photocurrents were recorded using borosilicate suction pipettes with a final tip diameter in the range of one-half of the cell diameter (i.d.) (Harz et al., 1992; Holland et al., 1996). The pipettes had an access resistance of 20–50 MΩ. Cells were sucked into the pipette by up to 50% until the resistance reached 60–150 MΩ. Under these experimental conditions, ~33% of the total current can be detected (Holland et al., 1996). Currents were recorded at constant voltage (0 mV between bath and pipette) and were filtered with a 3 kHz low-pass Bessel filter. Data were recorded with a sampling rate of 10–100 kHz and processed as described by Harz et al. (1992). If not otherwise indicated, the current traces shown are the mean of 10 individual recordings filtered with a digital Gaussian filter to 1 kHz. The orientation of the cells was not optimized for maximal light sensitivity as described before by Harz et al. (1992).

Patch pipette measurements

Pipettes for measuring I_Ps directly at the eyespot were pulled from borosilicate glass capillaries (1.8 mm o.d., 0.15-mm walls, Kimax-51, Witz Scientific, Maumee, OH) in two steps and were polished until the tip diameter reached ~1.5 μm. The cone angle was ~30°. The pipettes were filled with and cells were incubated in NMG^+/K^+-buffer for I_P measurements. The resistance of the pipette was 15–20 MΩ. When the region of the cell containing the eye (diameter ≈ 1.5 μm) was sucked into the pipette, the resistance increased to 120–160 MΩ. A 40x objective (*na* = 1.3, Achrostigmat, Zeiss, Oberkochen, Germany) and a 4x phototube were used for identifying the eyespot by infrared light on the monitor (Holland et al., 1997).

Cells were stimulated through the objective by a 10-μs flash (500 nm, 60 nm half-bandwidth). Complete (100%) photon exposure corresponds to 1.563 μE m^{-2} in the objective plane. Light pulses (500 nm, 60 nm half-bandwidth) had a duration of 300 ms and were controlled by a fast electronic shutter. Complete (100%) photon irradiance corresponds to 38.6 mE m^{-2} s^{-1}. Measurements were carried out at room temperature (20°C).

Action spectra

Action spectra for I_{P1b} and I_{P2b} were obtained by evaluating data from at least three different cells (Harz and Hegemann, 1991). The linear part of the stimulus-response curves (peak current vs. log Q) was extrapolated to zero. The absolute light sensitivities (1/threshold photon exposure) as determined for six different wavelengths were normalized to the 510-nm value and plotted versus wavelengths.

Reaction scheme

The numerical values given here refer to Rh_b There are 10^4 *Rh* molecules in the eye (Beckmann and Hegemann, 1991). In the unilluminated eye all *Rh*s are in the inactive ground state *I*. Upon illumination with *L* photons per *Rh* in a 10-μs flash, part of *I* (*L* times $\Phi \cdot \sigma = 10^{-20} \cdot 0.7$) will be converted to the first non-excited state *K* with the apparent rate constant $L \cdot k_{IK}$ (k_{IK} = 1000 s^{-1}/L); *K* will fall back to the dark state *I* through a cascade of intermediate states (in further alphabetical order), *L*, *M*, *N*, *O*, and *P*, with the corresponding rate constants k_{KL} 200, k_{LM} 3000, k_{MN} 500, k_{NO} 100, k_{OP} 20, and k_{PI} 10 s^{-1}. The state *M* permits 0.01 pA Ca^{2+} inward current per Rh/G_{1b} unit, with 0.01 mM half-saturating $[Ca^{2+}]_o$, and the state *O* a H^+ entry by a constant field H^+ conductance G_H of 2 $pSmM^{-1}$.

After illumination, the currents through *M* and *O* will change the voltage in the area of the membrane enclosing the eye and will thus alter the driving forces in the equivalent circuit. These changes can be calculated by numerical integration.

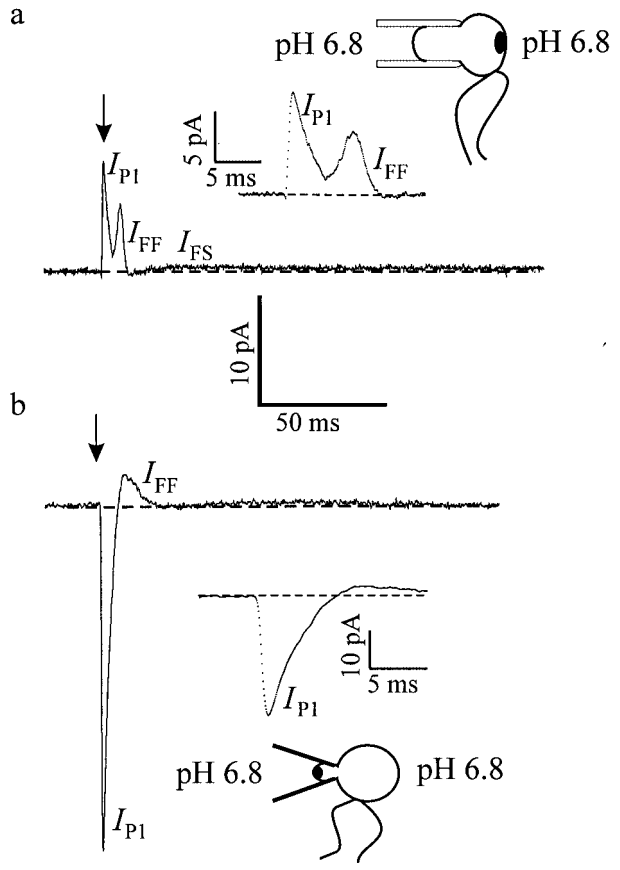

FIGURE 2 Two representative current records in response to a saturating light flash under different measuring configurations. (*a*) Suction pipette measurement with eyespot and flagella exposed to the bath medium. (*b*) Patch pipette measurement with eyespot in the pipette.

RESULTS

Classification of flash-induced transient inward currents

For an overview and for reference purposes, Fig. 2 shows typical current tracings as recorded from *C. reinhardtii* upon stimulation with short light flashes. In the experiment of Fig. 2 *a* the cell was sucked into a suction pipette with both eye and flagella exposed to the bath medium, whereas in Fig. 2 *b* the eye was sucked into a patch pipette with small tip diameter and steep cone angle. The suction mode (*a*) allows the recording of the photoreceptor currents I_P and flagellar currents, I_F, (Litvin et al., 1978; Harz and Hegemann, 1991). Photoreceptor currents have been defined in the past as eyespot-localized currents, whereas flagellar currents are distributed along the whole flagella (Beck and Uhl, 1994). Under the configuration with the eyespot facing the bath compartment, all currents are only ~25% of the total (Holland et al., 1996). In contrast, patch pipette experiments with the eyespot in the pipette allow the recording of 80% of I_P, whereas the flagellar currents are generally much smaller (Fig. 2 *b*). The I_P sign inversion is attributable to the current vectors, i.e., either from the bath into the eye (*a*) or from the pipette into the eye (*b*), respectively.

In this report we will present data about a second photoreceptor current I_{P2}, which follows I_{P1} when $[H^+]_o$ at the eye is high enough. Before presenting details of the novel event I_{P2}, we examine the hypothesis that the well-known current I_{P1} consists of two distinct components. Photoreceptor currents recorded at a few selected photon exposures are shown in Fig. 3 *a*. In Fig. 3 *b*, the peak current of I_{P1} is plotted versus the photon exposure of the actinic flash. This experimental relationship is well fitted by the sum of two hyperbolic Michaelis-Menten-type kinetic components (relative deviation from solid line: 0.6 pA):

$$I_{P1}(Q) = I_{Sa}/(1 + Q/Q_{1/2a}) + I_{Sb}/(1 + Q/Q_{1/2b}) \quad (1)$$

with the saturating amplitudes $I_{Sa} = 4.85$ pA and $I_{Sb} = 38.36$ pA, and the half-saturating photon exposures $Q_{1/2\ a} = 0.14$ and $Q_{1/2\ b} = 57.72\ \mu E\ m^{-2}$ of the two respective components. The line in Fig. 3 *c* represents an alternative fit with the sum of two exponentials,

$$I_{P1}(Q) = I_a(1 - \exp(-Q/Q_a)) + I_b(1 - \exp(Q/Q_b)). \quad (2)$$

which resulted in an inferior approximation, especially for low photon exposures attributable to the stronger curvatures in exponentials compared with hyperbolas (relative deviation from the solid line: 1.3 pA).

I_{P2}: Light-induced H^+ entry

The novel phenomenon reported here is I_{P2}, a flash-induced, slow, transient, inward current through the eye region. I_{P2} is virtually absent at pH 6.8 (Fig. 2) but is clearly visible at pH 4.0 (Fig. 4, *a* and *b*). The magnitude of I_{P2} has been titrated with respect to the pH in the eye region. For this purpose we did not simply pick the peak of I_{P2} which may be distorted by the flagellar currents I_{FF} between I_{P1} and I_{P2}. Rather, we picked I_{P2} 100 ms after the flash, when I_{FF} has decayed. These values of $I_{P2,100ms}$ have been related to the peak of I_{P1}, the latter being independent of pH. Fig. 4 *c* shows an example of a resulting Lineweaver-Burk plot of $I_{P1,\ peak}/I_{P2,100ms}$ versus $1/[H^+]$. These straightforward Michaelis-Menten kinetics indicate that I_{P2} is carried by H^+. However, strictly speaking, such kinetics might also be brought about by H^+ gating of a non-H^+ conductance. Means from $n = 7$ independent cells are $-1/K_m = 4.06 \pm 0.26\ mM^{-1}$ and $(I_{P2,100\ ms}/I_{P1,peak})_{max} = 0.93 \pm 0.22$. Corresponding kinetic evidence for I_{P1} being carried by Ca^{2+} is not available. Nevertheless, this strong kinetic evidence in Fig. 4 *c* is not absolutely compelling. There is still a possibility that H^+ has only a catalytic effect on I_{P2}. Usually, this discrimination can be made in thermodynamic terms through the

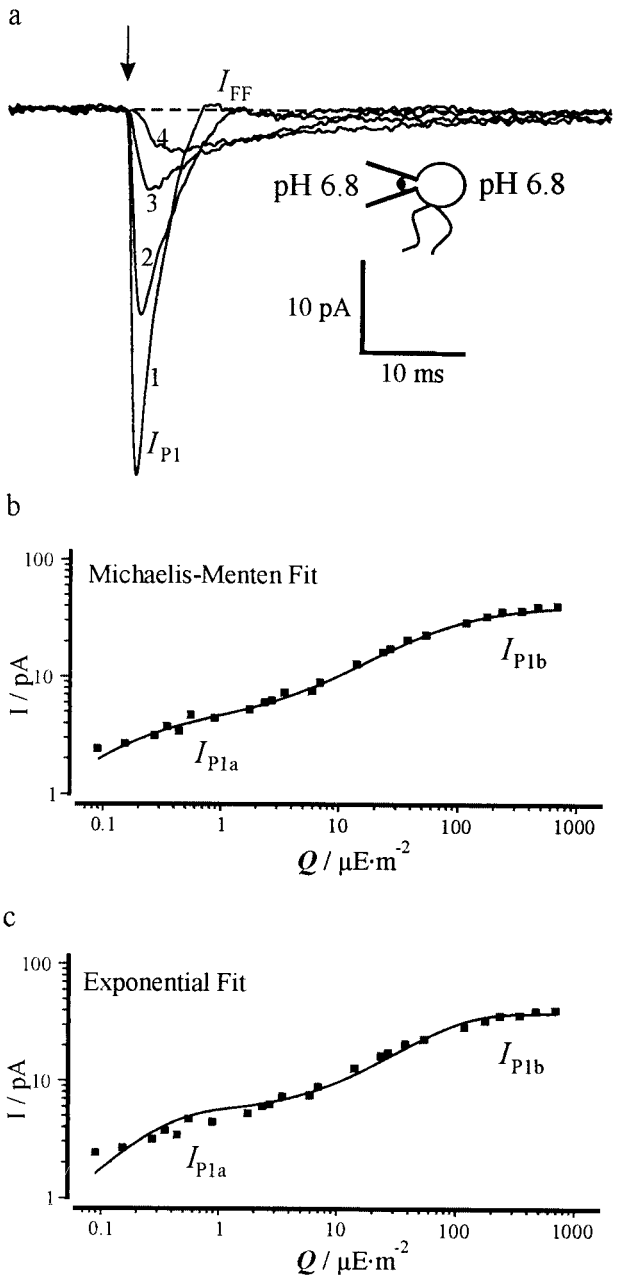

FIGURE 3 Light dependence of the peak amplitude of I_{P1a}+ I_{P1b}. (*a*) Four representative traces recorded at 1:690; 2:54; 3:6.9; and 4:0.55 μE m^{-2}. (*b* and *c*) The peak amplitude is plotted vs. the photon exposure of the actinic light flash; lg/lg plot; *points*, data; *lines*, theoretical approximations (fits). (*b*) Solid line represents the sum of two Michaelis-Menten components: I_{P1} (Q) = $I_{Sa}/(1 + Q/Q_{1/2a}) + I_{Sb}/(1 + Q/Q_{1/2b}$) with fitted values of I_{Sa} = 4.85 pA $Q_{1/2a}$ = 0.14 μE m^{-2}, I_{Sb} = 38.36 pA, and $Q_{1/2b}$ = 57.72 μE m^{-2}. (*c*) Sum of two exponentials: $I_{P1}(Q) = I_a(1 - \exp(-Q/Q_a)) + I_b(1 - \exp(Q/Q_b)$ with fitted values of I_a = 4.01 pA, Q_a = 0.27 μE m^{-2}, I_b = 31.72 pA, and Q_b = 80.93 μE m^{-2}

Nernst equation and reversal voltage. Unfortunately, this approach is not technically feasible in our system because the membrane voltage is not accessible.

Low $[K^+]_o$ promotes I_{P2}

Taking I_{P2} for a proton current, I_H, led to the expectation that its size does not depend on the osmotic component, ΔpH, of the *pmf* alone. The transmembrane voltage, V_m, as the electrical component of the *pmf* should have an equivalent influence. Unfortunately, corresponding V-clamp experiments can not be performed in *C. reinhardtii* at the moment. However, predominant K^+ diffusion is common in biological membranes, including the plasma membrane of *C. reinhardtii* (Malhotra and Glass, 1995). Thus, we expected that $[K^+]_o$ influences V_m according to the Nernst equilibrium voltage for K^+, $E_K \approx (-59$ mV)lg($[K^+]_i/[K^+]_o$), and the H^+-inward current I_{P2}.

These relationships were investigated by the experiments presented in Fig. 5. In the given configuration, the large membrane portion in the bath will guarantee a high impact of $[K^+]_o$ on the uniform, internally short-circuited V_m. This means that in the experiment depicted in Fig. 5 *a*, V_m was presumably rather negative because of the low $[K^+]_o$ in both compartments. Upon exposure of the predominant membrane portion in the bath to high $[K^+]_o$, V_m was presumably also less negative in the membrane region within the pipette not directly exposed to high $[K^+]_o$. This intended manipulation of V_m resulted in the expected reduction of $I_{P2} \approx I_H$. As seen from the graph in Fig. 5 *b*, 10 mM $[K^+]_o$ inhibits I_{P2} by 50%, and >20 mM $[K^+]_o$ in the bath causes K^+ to move from the bath compartment through the cell into the pipette (I_K in Fig. 5 *a*). The large I_{P2} and the dependence on $[K^+]_o$ are consistent with the gating properties of the K^+ outward-rectifying channels (Blatt and Gradmann, 1997) that seem to be ubiquitous in plant cells. A transient depolarization from a pump-dominated, negative resting voltage V_r (here ≈ -150 mV) will cause a transient activation of these channels which results, at 1 mM $[K^+]_o$, in an accelerated repolarization toward E_K (Govorunova et al., 1997). At $[K^+]_o$ >10 mM, the repolarization is inhibited and the driving force for H^+ flux at acidic pH is suppressed; the small outward current observed at pH 6.8, 50 ms after flash (Fig. 5 *b*) is not affected by high $[K^+]$ in the bath.

It is noted that this effect of V_m on I_H is not specific; rather, it applies for the inward currents of any ion at physiological driving forces ($V - E_X$) < 0. Transcellular currents at asymmetric $[K^+]_o$ also accompany the large flagellar currents observed at high Ba^{2+} concentration (Nonnengäβer et al., 1995).

I_{P1} and I_{P2} depend on $[Ca^{2+}]_o$

The high light-saturating component of I_{P1}, I_{P1b}, has been known to be carried by Ca^{2+} (Sineshchekov, 1991; Holland et al., 1996), whereas the ionic nature of the smaller, low light-saturating component I_{P1a} was not yet known. To isolate the inward currents I_{P2} from I_{P1}, we intended to

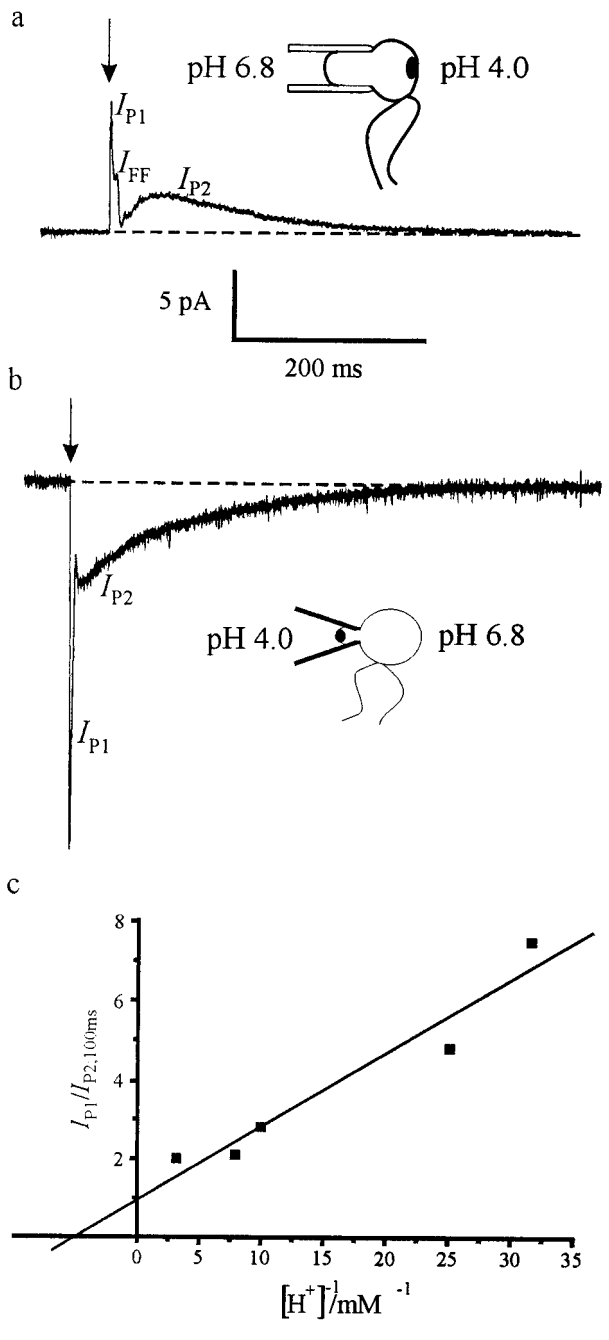

FIGURE 4 (*a* and *b*) Transient inward currents through the eye of *C. reinhardtii* upon short light flashes, recorded under different pipette configurations with pH_o 4 in the compartment of the eye and 200 μM Ca^{2+} in both compartments. (*c*) The influence of $[H^+]_o$ on the second photocurrent, $I_{P2,}$ of a typical cell is shown in a Lineweaver-Burk plot; data were sampled 100 ms after the flash (not peak) and related to peak of I_{P1}. Mean values of seven cells are discussed in the text.

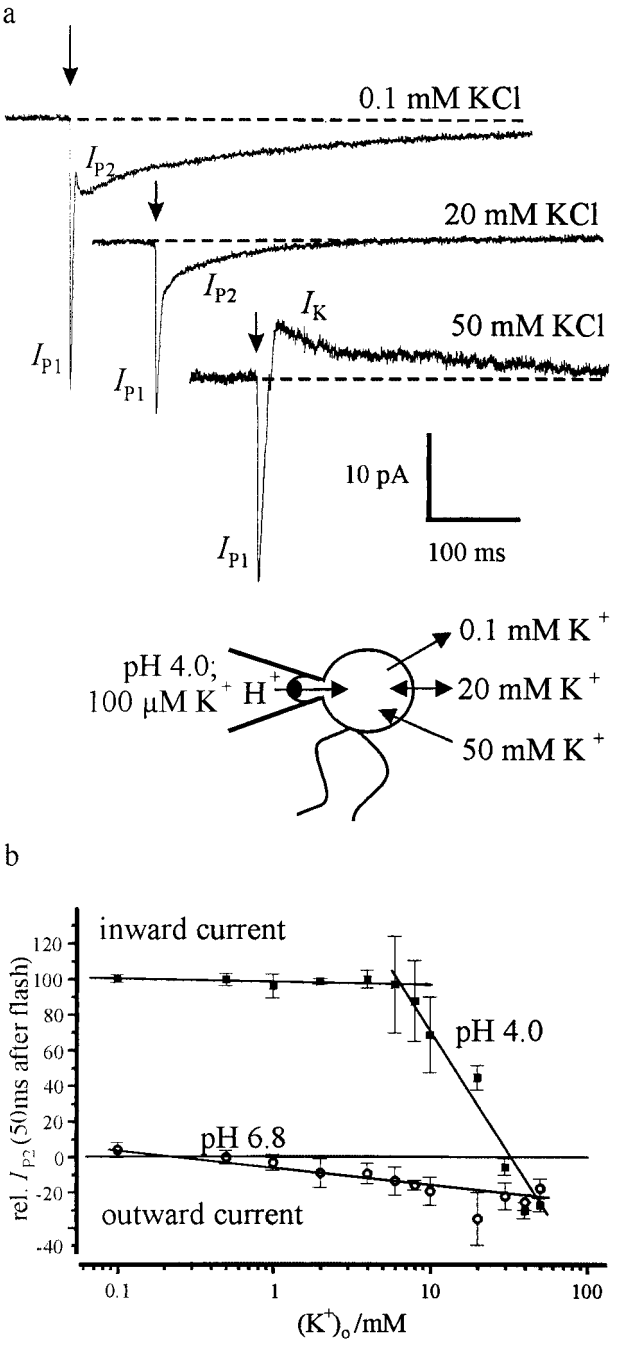

FIGURE 5 Influence of external K^+ on early and late flash-induced inward currents, I_{P1} and I_{P2}, through the eye. (*a*) Three representative traces at three different K^+-concentrations in the bath medium. Note that 50 mM K^+ leads to an inversion of the I_{P2} signal, whereas I_{P1} remains almost unchanged. (*b*) Plot of the current amplitudes 50 ms after the flash vs. the K^+ concentration in the bath compartment (the lines are drawn to guide the eye).

record I_{P2} at low $[Ca^{2+}]_o$. At acidic pH, a defined $[Ca^{2+}]_o$ can not be adjusted in the usual way by buffering Ca^{2+} with common chelating agents because the carboxyl groups of EDTA or BAPTA are protonated at acidic pH. Therefore, the cells were repeatedly washed with ultrapure 100 μM KPi-buffer that contained ~1 nM Ca^{2+}. Measurements were carried out in this low ionic-strength buffer, and the cell was decoupled from the Ag/AgCl electrodes by salt

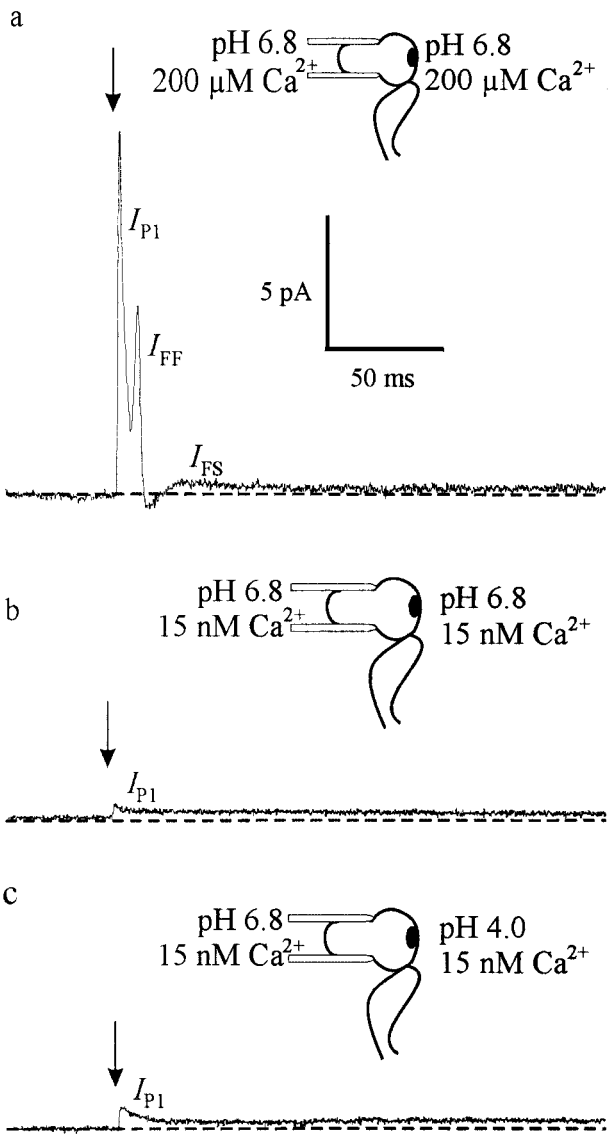

FIGURE 6 Low extracellular Ca^{2+} suppresses I_{P1} and I_{P2}. Measuring KPi-puffer including 200 μM Ca^{2+} (*a*) was replaced by deionized KPi with 15 nM Ca^{2+} and pH 6.8 (*b*) or pH 4.0 (*c*).

bridges as explained in Fig. 1. Under reference conditions (Fig. 6 *a*) with 200 μM $[Ca^{2+}]_o$ in phosphate buffer of pH_o = 6.8, I_{P1} had its usual size. When cells of the same batch were tested in Ca^{2+}-depleted phosphate buffer (15 nM final concentration), I_{P1} was almost absent, indicating that not only I_{P1b} but also I_{P1a} is suppressed. Moreover, after acidification of the bath compartment toward pH 4.0, no I_{P2} could be evoked either, which is a strong indication that all three photoreceptor current components are in some way Ca^{2+}-sensitive. It should be pointed out that, compared with all former experiments, the bath medium in the experiment to Fig. 6, *b* and *c* was also Cl^--depleted. But, addition of Cl^- did not restore I_{P1} or I_{P2}.

Light dependence of I_{P2}

The similar response of I_{P1} and I_{P2} to depletion of external Ca^{2+} (Fig. 6) may suggest coupling between these two events. An equivalently close relationship between these two currents exists with respect to their light dependence. The dependence of I_{P1} on the photon exposure provided by individual flashes has already been presented in detail in Fig. 3. Fig. 7 shows this dependence for eyespot in conditions and pH 4.0 in the pipette. The peak amplitude of I_{P2} throughout is ~20% of that of I_{P1} at all flash-conditions tested. I_{P1} and I_{P2} increase in parallel with the flash photon exposure between 6.2 and 1250 μE m^{-2}. Again, like the saturation curve for I_{P1} at pH 6.8, both curves for I_{P1} and I_{P2} are too flat to be described by a single Michaelis-Menten or a single exponential saturation curve. Two Michaelis-Menten curves shown in Fig. 7 *c* describe the data for acidic conditions adequately.

Using common $Q_{1/2a}$ and $Q_{1/2b}$ for grouped fits of $I_{P1}(Q)$ and $I_{P2}(Q)$ with Eq.(1) resulted in $Q_{1/2a}$ = 1.52 and $Q_{1/2b}$ = 136.24 μE m^{-2} for photocurrents at acidic conditions. This supports the close relationship between I_{P1} and I_{P2}. The resulting amplitudes are: I_{P1a}, 3.03 pA; I_{P1b}, 31.32 pA; I_{P2a}, 0.31 pA; and I_{P2b}, 7.58 pA.

In addition, in both time courses, $I_{P1}(t)$ and $I_{P2}(t)$, the times t_{P1} and t_{P2} between light flash and current peak (flash-to-peak time, t_{ftp}) contract with increasing light intensity toward a discrete minimum ($t_{P1,min} \approx 1$ ms, $t_{P2,min} \approx 3$ ms) (Fig. 7 *d*). However, the I_{P1} peak times of the *a* and *b* components overlap over wide range of photon exposure, whereas those of *a* and *b* of I_{P2} are more clearly separated with a clear switch near 25 μE m^{-2} s^{-1}. The change of the flash-to-peak-time is not trivial because in a simplistic model with defined signal transduction mechanism light affects only the prime reaction step of photoconversion and, in the following reactions, only the amplitudes, but not the time courses, are affected by the light intensity. Because the light sensitivity of $I_{P1}(t)$ and $I_{P2}(t)$ differs from this simplistic pattern in the same fashion, a close mechanistic relationship between I_{P1} and I_{P2} can be inferred (further discussion below).

Stimulus-response curves for the range between 10 and 90% saturation where I_{P1b} and I_{P2b} dominate the photocurrents were recorded for different wavelengths. The amplitudes were plotted versus log Q and extrapolated to zero. The sensitivity defined as 1/threshold was plotted versus the wavelength and the resulting action spectra for I_{P1b} and I_{P2b} at pH 4 are seen in Fig. 7 *b*. Both spectra are compared with a standard rhodopsin nomogram (Knowles and Dartnall, 1977). The shape and the peak at 500 nm are nearly identical to the earlier presented action spectrum for I_{P1b} recorded at neutral pH (Harz and Hegemann, 1991). The close agreement between the data and the nomogram leaves little doubt that the photoreceptor for I_{P2b} is also a rhodopsin.

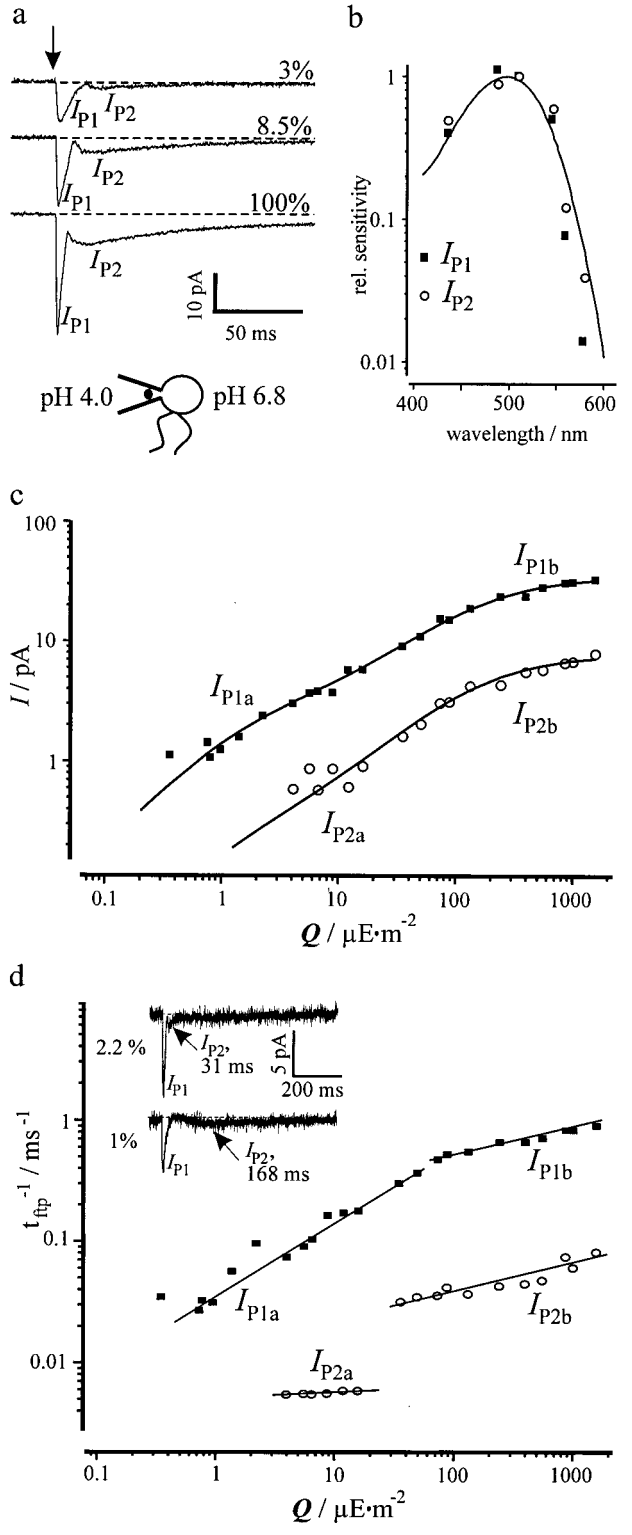

FIGURE 7 Dependencies of amplitudes and temporal responses of I_{P1} and I_{P2} on photon exposure, Q, of the light flash. (*a*) Selected current recordings at three selected photon exposures (10% = 156 μE m^{-2}). (*b*) Action spectra for I_{P1b} and I_{P2b} constructed from stimulus response curves as described in Material and methods. The solid line shows a standard rhodopsin spectrum taken from Knowles and Dartnall (1977). (*c*) Peak amplitudes of I_{P1} and I_{P2} plotted vs. the flash photon exposure Q. The data for the grouped fit for photocurrents at acidic conditions are: $Q_{1/2\ a} = 1.52$ and $Q_{1/2\ b} = 136.24$ μE m^{-2}. The resulting amplitude values are: $I_{P1a} = 3.03$ pA; $I_{P1b} = 31.32$ pA; $I_{P2a} = 0.31$ pA; and $I_{P1b} = 7.58$ pA. (*d*) Plot of the reciprocal flash-to-peak-times (t_{fip}^{-1}) vs. the flash photon exposure Q.

Step responses

To inquire to what extent the photocurrents in continuous light are carried by H^+, responses to step-up stimulation were analyzed at different pH. From responses to on- and off-steps of light we expected a distinction between transient and permanent components. For this purpose, light pulses of 300 ms were applied in a separate set of experiments. At pH_o 6.8 at the eye region, transient current peaks provisionally assigned as I_{P1} and I_{FF} are followed by a small stationary current of 1 to 2 pA (Fig. 8 *a*). I_{FF} is an all-or-none response and it disappears when the flagella are chopped off (data not shown), which justifies its assignment as a fast flagellar current corresponding to I_{FF} in flash experiments. Stationary photocurrents were observed before in *H. pluvialis* (Sineshchekov, 1991), but because of the small amplitude they have never been investigated systematically.

Upon acidification of the eye region we expected additional current responses related to I_{P2}. Fig. 8 *b* shows such additional responses, which consist of a second transient, peaking at ~ -9 pA some 50 ms after light-on before it decays with $\tau \approx 100$ ms to a stationary level, I_{SS}, of ~ -7 pA under maximum (100%) step-illumination. Upon turning the light off, the current decays with only one predominant exponential ($\tau \approx 200$ ms). At lower intensities (<15% light) we noticed that the slow and transient peak I_{P2} vanishes and the stationary level is apparently reached with one exponential ($\tau \geq 120$ ms). However, the light-off response now shows two exponential components, e.g., the 26% response in Fig. 8 *b*, a fast one ($1/\tau \approx 25$ s^{-1}) with an amplitude $A_1 \approx 1$ pA and a slow one ($1/\tau \approx 2.5$ s^{-1}) of a similar amplitude $A_2 \approx 1$ pA. Comparing the tracings in Fig. 8 *b* shows that the fast off-component (τ_1) becomes smaller with decreasing intensity of the preceding continuous illumination. Thus, we may conclude that at 100% light in Fig. 8 *b* the stationary current is mainly attributable to the high saturating component G_{2b}, whereas G_{1a}, G_{2a}, and G_{1b} significantly contribute at lower but more physiological intensities. Unfortunately, the rise of I_{P2} is disturbed by the positive I_{FF}, precluding a more detailed analysis.

A systematic evaluation of these features from three experiments over an intensity range of more than two orders of magnitude is illustrated by Fig. 9. The two current transients I_{P1} and I_{P2} and the stationary current I_{SS} increase more or less in parallel with the intensity of the light (Fig. 9 *b*). Above 10 mE m^{-2} s^{-1} the new transient I_{P2} is distinct from I_{SS}. Because I_{P2} and I_{SS} are

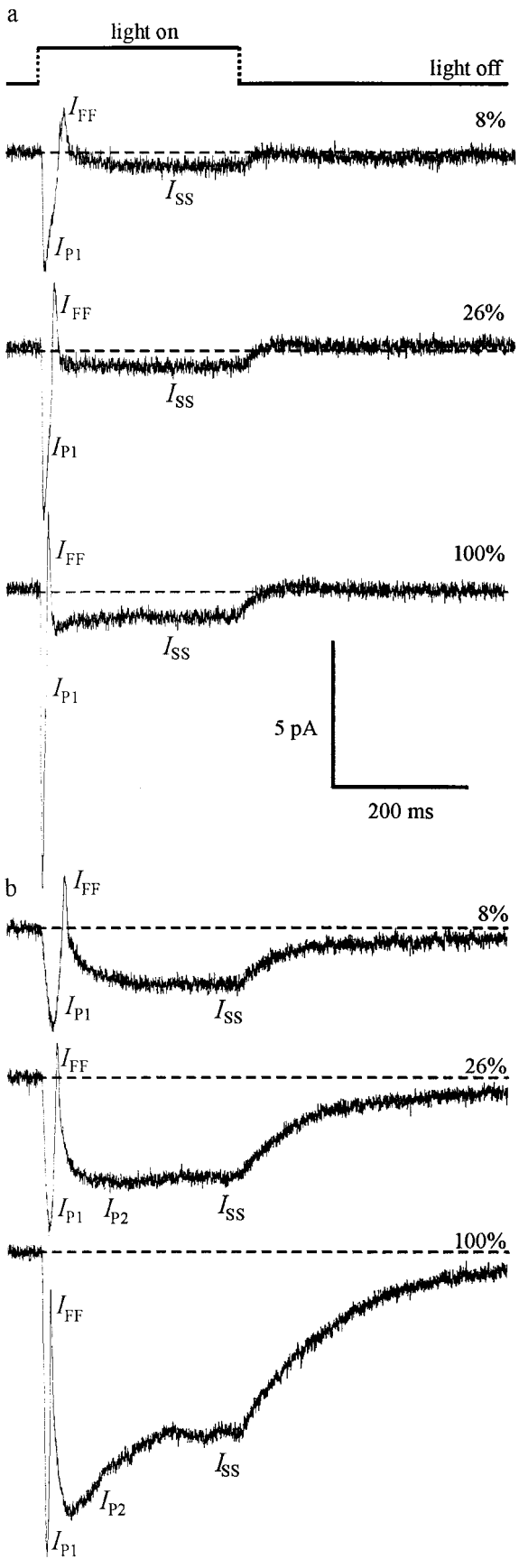

FIGURE 8 pH- and intensity-dependence of temporal responses of I_P upon light-on and -off. Currents traces were recorded in response to step-up and down stimulation at pH 6.8 (*a*) and pH 4.0 at the eye (*b*); 100% = 40 μE m^{-2} s^{-1}.

only visible or largely enhanced at low pH, we anticipate that both mainly reflect H$^+$-carried I_{P2} (*a* and *b*), discussed extensively above. The step-up-to-peak time, t_1, is shortened at higher light intensities. The peak I_{P2} appears only at high irradiance, whereas two exponential components $A_1\exp(-t/\tau_1)$ and $A_2\exp(-t/\tau_2)$ in the relaxation of $I_P(t)$ from I_{SS} to zero after light-off become most clearly visible after moderate irradiance $\leq$ 10 mE m^{-2} s^{-1} (26% in Fig. 8 *c*). Owing to the fact that I_{P1} is quite independent of the extracellular pH and rapidly decays after a flash, we assume that the conductances G_{1a} and G_{1b} define the small stationary current seen at pH 6.8, but hardly contribute to the stationary current observed at acidic pH. In line with this conclusion we assigned the components contributing to I_{SS} to a slow, high-sensitivity component, I_{P2a}, and to a fast, low-sensitivity component, I_{P2b}, of H$^+$ current with the relaxation constants $1/\tau_{P2a} = {\tau_2}^{-1}$ and $1/\tau_{P2b} = {\tau_1}^{-1}$, respectively (Fig. 9, *b* and *c*).

DISCUSSION

The four eyespot photoreceptor currents I_{P1a}, I_{P1b}, I_{P2a}, I_{P2b}

At neutral pH, all eyespot-restricted photocurrents appearing in *C. reinhardtii* after a flash or upon step-up stimulation are sufficiently explained by two light-induced conductances, G_{1a} and G_{1b}. The few studies carried out previously on I_{P1} in the green algae *C. reinhardtii* and *H. pluvialis* have generally focused on the fast high-light saturating component I_{P1b}. This major photoreceptor current was proposed to result from a conductance (G_{1b}), that is closely coupled to rhodopsin (Harz et al., 1992). A large body of evidence has accumulated showing that the I_{P1b}-induced depolarization triggers the flagellar currents, I_{FF}, that, in turn, cause a switch from forward to backward swimming (Holland et al., 1997). The other component of I_{P1}, I_{P1a}, saturating at low light has not been studied in detail because of its small amplitude. It was not clear which ion was the carrier of I_{P1a} because adjustment of Ca^{2+} in the medium by EDTA or BAPTA did not reduce I_{P1} below 15% of its full size (Sineshchekov, 1991; Holland et al., 1996). We have shown above that a careful removal of Ca^{2+} by an ion exchanger also suppresses I_{P1a}. In earlier experiments, Ca^{2+} might not have been removed completely from the inner cell wall layer that is still present in the cell wall-deficient CW2 mutant. The possibility has been under discussion for years that a low-saturating photoreceptor current, here named I_{P1a},

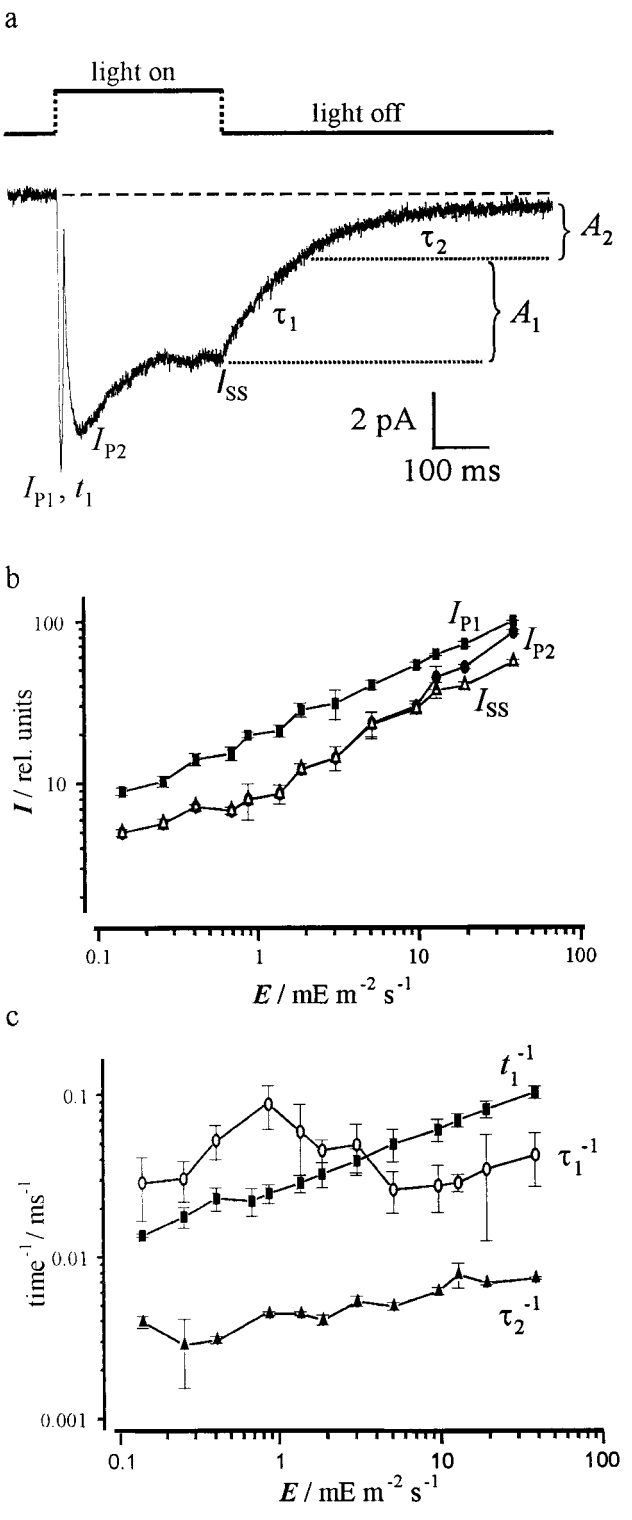

FIGURE 9 Synopsis of changes in characteristic parameters in step response of light-induced inward currents across the eyespot overlaying part of the plasmalemma as functions of the intensity of the 300-ms pulse of light. (*a*) Typical current trace and the parameters that were evaluated. (*b*) Double logarithmic plot of the three current amplitudes I_{P1}, I_{P2}, and I_{SS}. (*c*) Double logarithmic plot of the step-up to peak time t_1^{-1}, and the two decay times after light off, τ_1^{-1} and τ_2^{-1}.

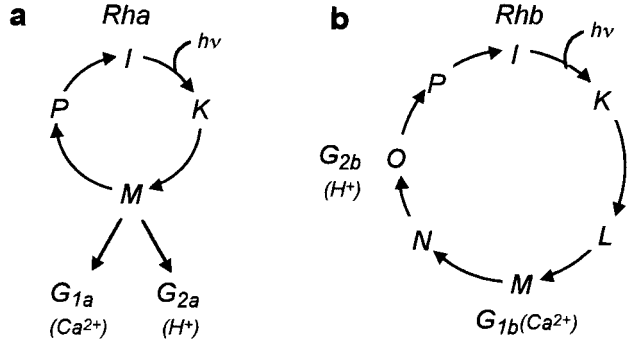

FIGURE 10 Schematic representation for the activation of light-induced conductances in the *C. reinhardtii* eye by two rhodopsins, Rha and Rhb. (*a*) Rha activates G_{1a} within 1 ms and G_{2a} within >100 ms via a side reaction starting from the intermediate *M*. The activation of G_{1a} and G_{2a} might occur in sequence or via different pathways (as shown here). (*b*) Simplified cyclic reaction cycle used for the calculation of the high-light saturating photocurrents mediated by Rhb and two conductances, G_{1b} and G_{2b}. The delay for the activation of the Ca^{2+} conductance G_{1b} only a few microseconds and the I_{p1b} maximum is reached within 1 ms (flash-to-peak), whereas that of the H^+ conductance G_{2b} is reached only after >5 ms.

triggers distinct direction changes in response to flashes or phototaxis in continuous light. This current has not yet been characterized, and the mechanism through which it might induce direction changes is still obscure. The new finding at least is consistent with the decade-old knowledge that phototaxis is a strongly Ca^{2+}-dependent process (Stavis and Hirschberg, 1973), supporting the hypothesis that I_{P1a} serves as a trigger for direction changes and phototaxis. It should also be clear now that I_{P1a} involves a multicomponent signaling system, the saturation of which is described by a low light-saturating Michaelis-Menten kinetics.

The stimulus/response relationship of a *n*th order reaction has the linear slope $m = n$ in the low-dose range of a lg/lg plot. This means that in this range, far from saturation, the observed linear slopes with $0 < m < 1$ can not be explained without additional assumptions. However, apparent slopes $0 < m < 1$ are frequently observed in lg/lg plots of biological dose-effect relationships, such as Figs. 3 *b* and 7 *c*. Stimulus-response curves with such small slopes provide the physiological benefit of covering a wide sensitivity range with a finite modulation depth of the sensor. This can not be realized by any signaling system that is simply proportional to the fraction of photoreceptor bleaching. The fact that the data in Figs. 3 *b* and 7 *c* are fitted well by two kinetic components suggests the operation of two kinetic systems with sensitivity ranges that differ by approximately a factor of 100: a high-sensitivity system (*a*) and a low-sensitivity system (*b*).

Owing to the fact that I_{P1a} and I_{P2a} saturate at low photon exposures and occur with millisecond delays after flash (Braun and Hegemann, 1999a), we suggest that the responsible rhodopsin evokes the two conductances G_{1a} and G_{2a} via a transmitter (Fig. 10 *a*). In contrast, the simplest ex-

planation for the low sensitivity system is a single-reaction cycle of a protein complex including rhodopsin and two conductances, G_{1b} and G_{2b}, as shown in Fig. 10 *b*. In this reaction scheme, a defined 1:1 stochiometry between rhodopsin and each conductance is anticipated without specifying how many proteins are involved. The cyclic reaction sequence shown in Fig. 10 *b* is intended to explain qualitatively the kinetics of the two photocurrents I_{P1b} and I_{P2b} at a given high photon exposure. The reaction cycle comprises seven states and transitions of the rhodopsin/ion channel complex. The numbering is in alphabetical order starting with the inactive, resting state *I*. In the scheme the states *M* and *O* represent the conducting states $G_{1b}(Ca^{2+})$ and $G_{2b}(H^+)$, respectively. *K* does not directly convert into *M* because the rise of *M* occurs with a delay of several microseconds (Holland et al., 1996; Braun and Hegemann, 1999a), whereas the lifetime of *K* should be in the nanosecond range. Similarly, *M* does not directly convert into *O* because the decay of I_{P1} is faster than the rise of I_{P2}. This purely sequential model is consistent with the observed sequential appearance of I_{P1b} and I_{P2b} and with their light saturation in parallel with rhodopsin bleaching.

It had been previously noted on studies on *H. pluvialis* (Sineshchekov et al., 1990) and *C. reinhardtii* (Harz et al., 1992) that the flash-to-peak time, t_{ftp}, depends on *Q*. This finding is surprising in terms of straightforward photochemistry, because the velocity of the reaction cascade after the initial and only photochemical excitation is expected to be independent to the light intensity. If we assign different velocities of the cascades in systems *a* and *b*, superpositions of the current transients from the two systems, *a* and *b* of Fig. 10, will cause apparent dependencies of t_{ftp} on *Q*. Systematic investigation of this relationship on *C. reinhardtii* and *V. carteri* shows that this dependency seems to be steeper in the low-intensity range than at high intensities as seen in Fig. 7 *d* (above) and in Fig. 4 of Braun and Hegemann (1999a). Moreover, the delay between flash and beginning of the I_{P1} also increases considerably at low light levels when the amplitude is relatively large compared with the fraction of rhodopsin bleached (Braun and Hegemann, 1999a). At high photon exposures, the behavior of the total system becomes simpler as the properties of the low-sensitivity system *b* predominate. Correspondingly, the gentle slopes of the $t_{ftp}(Q)$ relationships in the right part of Fig. 7 *d* are fairly consistent with the above notion that in a straightforward photoreceptor t_{ftp} is quite independent of *Q*.

In conclusion, at acidic pH, four distinct photoreceptor currents are identified in the eye of *C. reinhardtii*: the two early and probably Ca^{2+}-carried currents I_{P1a} and I_{P1b}, and the two late H^+ currents I_{P2a} and I_{P2b}. The same action spectra of I_{P1b} and I_{P2b} (Fig. 7 *b*) and the similar light dependence of the amplitudes (Fig. 7 *c*) and t_{ftp} (Fig. 7 *d*) suggest that the underlying conductances G_{1b} and G_{2b} are part of one reaction cascade *b*. The finding that G_{1a} saturates at ~100 times smaller light intensities than rhodopsin itself (e.g., Fig. 7 *c*) may be accounted for by the signaling cascade *a* (Fig. 10 *a*). The conductances G_{1a} and G_{2a} are activated when only 1% of the photoreceptor is excited. The number of channels might be smaller than that of the photoreceptor to explain the small maximal current I_{P1a}.

The responses of I_P on up- and down-steps of the quantum flux density *E* of various intensities, as summarized in Fig. 9, confirm the results of Fig. 7. The two time constants of the exponential current relaxation upon light off (τ_1 and τ_2 in Fig. 9, *a* and *c*) turned out to be insensitive to the intensity of the preceeding light (within the accuracy of the measurements, of course). They compare well with the t_{ftp} levels of I_{P2b} and I_{P2a} in Fig. 7 *c*, respectively. A quantitative analysis of the results of Figs. 7–9 by mechanistic models will be the subject of a separate study.

Geometric aspects

During the investigation of I_{P2} it was noticed that the recorded I_{P1} and I_{P2} were larger when the eye was in the pipette and the membrane portion in the pipette was small, compared with the configuration with the eye exposed to bath and a larger membrane portion outside the pipette (Figs. 2 and 4). This is attributable to the fact that in the configuration of Fig. 4 *a* only a fraction of the total current through the eye is recorded (Braun and Hegemann, 1999a). Correspondingly, the de- or hyperpolarizing effects of external anions (such as H^+ or K^+) on the resting voltage are expected to increase as the surface portion (bath/pipette) is exposed to changes in external ionic composition.

The number of photoreceptor species involved

As shown in the past by electrical measurements on single cells, the photocurrent I_{P1b} has a rhodopsin action spectrum peaking at 495 nm (Harz and Hegemann, 1991). Later, in populations of retinal-deficient cells that do not express any or extremely small photocurrents in response to light flashes, low- and high-intensity photoreceptor currents (I_{P1a} and I_{P1b}) were reconstituted after addition of exogenous retinal (Sineshchekov et al., 1994; Govorunova et al., 2001). Both findings taken together strongly suggest that I_{P1a} and I_{P1b} are both rhodopsin-mediated processes, although their $Q_{1/2}$ differ by two orders of magnitude of light intensity. Because of the extremely small amplitudes, reliable action spectra of the I_{P1a} could not be generated in earlier studies nor in this one. Motion analysis and light scattering experiments with white cells that were reconstituted with retinoids and analog compounds have shown a close similarity in the chromophore structural requirements of the two behavioral responses, i.e., phototaxis and photophobic responses (Hegemann et al., 1991; Lawson et al., 1991; Takahashi et al., 1991). However, when the dependence of the direction changes and the phobic responses were analyzed with the

help of Poisson statistics, the conclusion was drawn that both are independent processes and may be triggered by individual photon absorptions (Marwan and Hegemann, 1988). Moreover, competition experiments with a 13-*trans*-locked retinal analog supported this notion by suggesting that slight differences exist between the two responses at the level of their photoreceptor proteins (Zacks et al., 1993). Despite the similarity of the action spectra for all flash-induced behavioral responses respective shape and peak maximum, it is conceivable that I_{P1a} and I_{P1b} are controlled by two different rhodopsin species as expressed by the models of Fig. 10.

The next question to be discussed is whether G_{2a} and G_{2b} are also rhodopsin-activated conductances. The retinal dependence of I_{P2} could not be demonstrated because of the instability of white cells at low pH (data not shown). We presented evidence that G_{2a} and G_{2b} conduct H^+ and are distinct from the two Ca^{2+}-conductances G_{1a} and G_{1b}. As stated before, I_{P2b} shares important features with I_{P1b}, most prominently the high light saturation with $Q_{1/2}$ of 58 $\mu E \cdot m^{-2}$. Assuming common values of an absorption cross-section of $1.9 \cdot 10^{-20}$ m^{-2} and a quantum efficiency of 0.7 for all known rhodopsins ($\epsilon = 50\,000$ M^{-1} cm^{-1}), both I_{P1b} and I_{P2b} saturate almost with the rhodopsin bleaching. We argued before that this implies a 1:1 ratio between rhodopsin and the photoreceptor channels or an ion-conducting photocycle intermediate (Harz et al. 1992) (Fig. 10 *b*). This may not be completely true, because with a fixed rhodopsin/channel stochiometry, light saturation of I_{P1b} should follow an exponential saturation curve which it does not do perfectly (Fig. 3 *c*). A multimeric photoreceptor complex (Melkonian and Robenek, 1984) with negatively cooperative ion-conducting properties, however, may explain the slightly better fit of the I_{P1b} data to the Michaelis-Menten equation of Fig. 3 *b*. In addition, to cover a dynamic light intensity range of three log units, the unitary conductance of the I_{P1b} and I_{P2b} must be small. Finally, taking the similar action spectra of Fig. 7 *b* into account, we propose that I_{P1b} and I_{P2b} are components of the same rhodopsin that has two conductances, G_{1b} and G_{2b} (Fig. 10 *b*); these might be two conducting intermediates of one rhodopsin photocycle. A fast cycling of the rhodopsin complex within 100–300 ms elegantly explains the observed large stationary currents, as only a small fraction of rhodopsin is in an inactive state.

The characterization of I_{P1a} and I_{P2a} remains less complete. The major drawback is that high resolution action spectra are missing. The earlier shown retinal-dependence of I_{P1a} (Sineshchekov et al., 1994) and the rhodopsin action spectra for phototaxis and all flash-induced behavioral responses (Uhl and Hegemann, 1990) lead us to the conclusion that I_{P1a} and probably I_{P2a} are activated by the same photoreceptor as shown schematically in Fig. 10 *a*. This conclusion needs further verification.

Contribution of $[K^+]_o$

Finally, one could ask the question why I_{P2} is not seen at neutral pH. In earlier experiments we demonstrated that the change of the extracellular pH from 6.8 to 4.0 only altered the internal pH by 0.25 units from pH 7.48 to 7.23 (Braun and Hegemann, 1999b). Consequently, the pH-gradient increased from $\Delta pH = 0.68$ to $\Delta pH = 3.23$, which would explain the observed I_{P2} increase. Concomitantly, the membrane potential in *C. reinhardtii* should shift from -115 to -75 mV, reducing the driving force for H^+ accordingly (Malhotra and Glass, 1995). But, we argue, under conditions when only the eyespot region was exposed to high proton concentrations, the eyespot is exposed to a high H^+ driving force without strong depolarization. In contrast to this view, I_{P2} increased less than I_{P1} in the eyespot-in configuration compared to eyespot-out (Fig. 4) and completely disappeared at high K^+. To understand this finding, the counterbalancing K^+-efflux must be considered. The nonlocalized K^+ efflux is facilitated by a less negative membrane potential as it should be realized under eyespot-out conditions, where the majority of the cell surface is exposed to low pH. Thus, we conclude that at acidic pH I_{P2} is determined by the H^+ influx into the eyespot and by a counterbalancing K^+ efflux.

We thank Dr. Georg Nagel for helpful suggestions for measurements at low Ca^{2+}, and Dr. Carl M. Boyd for critical reading of the manuscript. This work was supported by grants of the Deutsche Forschungsgemeinschaft, the Fond der Chemischen Industrie to PH, and by a grant (I76 841) of the Volkswagen-Stiftung to DG.

REFERENCES

Beck, C., and R. Uhl. 1994. On the location of voltage sensitive calcium channels in the flagella of *Chlamydomonas*. *J. Cell Biol.* 125: 1119–1125.

Beckmann, M., and P. Hegemann. 1991. In vitro identification of rhodopsin in the green alga *Chlamydomonas. Biochemistry.* 30:3692–3697.

Blatt, M. R., and D. Gradmann. 1997. K^+-sensitive gating of the K^+ outward rectifier in *Vicia faba* guard cells. *J. Membrane Biol.* 158: 241–256.

Braun, F. J., and P. Hegemann. 1999a. Two independent photoreceptor currents in the spheroidal alga *Volvox carteri. Biophys. J.* 76: 1668–1678.

Braun, F. J., and P. Hegemann. 1999b. Direct measurement of cytosolic calcium and pH in living *Chlamydomonas reinhardtii* cells. *Eur. J. Cell Biol.* 78:199–208.

Foster, K. W., and R. D. Smyth. 1980. Light antennas in phototactic algae. *Microbiol. Rev.* 44:572–630.

Govorunova, E. G., O. A. Sineshchekov, and P. Hegemann. 1997. Desensitization and dark recovery of the photoreceptor current in *Chlamydomonas reinhardtii. Plant Phys.* 115:633–642.

Govorunova, E. G., O. A. Sineshchekov, W. Gärtner, A. S. Chunaev, and P. Hegemann. 2001. Photoreceptor currents and photoorientation in *Chlamydomonas* mediated by 9-demethylchlamyrhodopsin. *Biophys. J.* 81:2897–2907.

Harz, H., and P. Hegemann. 1991. Rhodopsin-regulated calcium currents in *Chlamydomonas*. *Nature* 351: 489–491.

Harz, H., C. Nonnengäβer, and P. Hegemann. 1992. The photoreceptor current of the green alga *Chlamydomonas*. *Phil. Trans. R. Soc. Lond. B.* 338:39–52.

Hegemann, P., W. Gärtner, and R. Uhl. 1991. All-*trans* retinal constitutes the functional chromophore in *Chlamydomonas'* rhodopsin. *Biophys. J.* 60:1477–1489.

Holland, E. M., F. J. Braun, C. Nonnengäβer, H. Harz, and P. Hegemann. 1996. The nature of rhodopsin triggered photocurrents in *Chlamydomonas*. I. Kinetics and influence of divalent ions. *Biophys. J.* 70:924–931.

Holland, E-M., H. Harz, R. Uhl, and P. Hegemann. 1997. Control of phobic behavioral responses by rhodopsin-induced photocurrents in *Chlamydomonas. Biophys. J.* 73:1395–1401.

Knowles, A., and H. J. Dartnall. 1977. Spectroscopy of visual pigments. In: The Eye, Vol. 2. H. Davson, editor. B:76 Academic Press, New York.

Lawson, M., D. N. Zacks, F. Derguini, K. Nakanishi, and J. L. Spudich. 1991. Retinal analog restoration of photophobic responses in a blind *Chlamydomonas reinhardtii* mutant: evidence for an archaebacterial-like chromophore in a eukaryotic rhodopsin. *Biophys. J.* 60:1490–1498.

Litvin, F. F., O. A. Sineshchekov, and V. A. Sineshchekov. 1978. Photoreceptor electric potential in the phototaxis of the alga *Haematococcus pluvialis. Nature.* 271:476–478.

Malhotra, B., and A. D. Glass. 1995. Potassium fluxes in *Chlamydomonas reinhardtii. Plant Physiol.* 108:1527–1536.

Marwan, W., and P. Hegemann. 1988. Single photons are sufficient to trigger movement responses in *Chlamydomonas reinhardtii. Photochem. Photobiol.* 48:99–106.

Melkonian, M., and H. Robenek. 1984. The eyespot apparatus of flagellated green algae: a critical review. *Progr. Phycol. Res.* 3:193–262.

Nonnengäβer, C., E. M. Holland, H. Harz, and P. Hegemann. 1996. The nature of rhodopsin-triggered photocurrents in *Chlamydomonas*. II. Influence of monovalent ions. *Biophys. J.* 70:932–938.

Rüffer, U., and W. Nultsch. 1990. Flagellar photoresponses of *Chlamydomonas* cells held on micropipettes. I. Change in flagellar beat frequency. *Cell Motil.* 15:162–167.

Sineshchekov, O. A. 1991. Photoreception in unicellular flagellates: bioelectric phenomena in phototaxis. *In* Light in Biology and Medicine, Vol. 2. R. H. Douglass, editor. Plenum Publishing, New York. 523–532.

Sineshchekov, O. A., and E. G. Govorunova. 1999. Rhodopsin-mediated photosensing in green flagellated algae. *Trends Plant Sci.* 4:58–63.

Sineshchekov, O. A., E. G. Govorunova, A. Der, L. Keszthelyi, and W. Nultsch. 1992. Photoelectric responses in phototactic flagellate algae measured in cell suspension. *J. Phototchem. Photobiol.* 13:119–134.

Sineshchekov, O. A., E. G. Govorunova, A. Der, L. Keszthelyi, and W. Nultsch. 1994. Photoinduced electric currents in carotenoid-deficient *Chlamydomonas* mutants reconstituted with retinal and its analogs. *Biophys. J.* 66:2073–2084.

Sineshchekov, O. A., F. F. Litvin, and L. Keszethely. 1990. Two components of the photoreceptor potential in phototaxis of the flagellated green alga *Haematococcus pluvialis. Biophys. J.* 57:33–39.

Stavis, R. L., and R. Hirschberg. 1973. Phototaxis in *Chlamydomonas reinhardtii. J. Cell Biol.* 59:367–377.

Takahashi, T., K. Yoshihara, M. Watanabe, M. Kubota, R. Johnson, F. Derguini, and K. Nakanishi. 1991. Photoisomerization of retinal at 13-ene is important for phototaxis of *Chlamydomonas reinhardtii:* simultaneous measurements of phototactic and photophobic responses. *Biochem. Biophys. Res. Commun.* 178:1273–1279.

Uhl, R., and P. Hegemann. 1990. Probing visual transduction in a plant cell. *Biophys. J.* 58:1295–1302.

Zacks, D. N., F. Derguini, and J. L. Spudich. 1993. Comparative study of phototactic and photophobic receptor chromophore properties in *Chlamydomonas reinhardtii. Biophys. J.* 65:33508–33518.